Received: August 27, 2024 | Revised: November 2, 2024 | Accepted: November 5, 2024

JOURNAL OF APPLIED RESEARCH ON SCIENCE AND TECHNOLOGY
JARST
INSTITUTE OF RESEARCH AND DEVELOPMENT
RAJAMANGALA UNIVERSITY OF TECHNOLOGY THANYABURI
ISSN ONLINE: 2773-9473
https://ph01.tci-thaijo.org/index.php/rmutt-journal

Design of a two-seater seaplane wing spar structure with composite materials

Phacharaporn Bunyawanichakul, Monchai Suraratchai and Narongkorn Krajangsawasdi*

Department of Aerospace Engineering, Faculty of Engineering, Kasetsart University, Bangkok 10900, THAILAND
*Corresponding author: narongkorn.kra@live.ku.th

ABSTRACT

A two-seater, mono-wing seaplane was initially developed for survey and rescue operations, with an empty weight of 470 kg and a maximum takeoff weight of 650 kg. Fiber-reinforced composite materials, consisting of fiber reinforcement and thermosetting polymer, were used in this airframe to reduce weight because the structural properties can be customized by adjusting the orientation of the fiber fabric layup and removing redundant material, which is impossible with metal. This paper presents a comprehensive overview of the design process for the aircraft's primary I-beam wing spar, employing composite material. Before conducting design calculations, it is critical to consider the variability of characteristics of composite materials caused by fabrication conditions such as temperature, humidity, and defects. As a result, it is imperative to conduct thorough testing of carbon fiber-reinforced composites following many different testing requirements. The coupon tests capture critical characteristics such as strength, stiffness, and Poisson's ratio across several orientations. The wing spar I-beam structure was subsequently developed with three primary considerations: stiffness (maximum deflection), strength, and stability (structural buckling). Following preliminary sizing of the I-beam wing spar, a simple initial layup was recommended, with primary loading in each component. The initial design was then subjected to a more detailed calculation using classical lamination theory, which took into account distributed load along the wing, spar taper, ply-drops along the span, and composite layup guidelines in order to reduce structural weight while ensuring the main spar's ability to withstand operational loads effectively. The calculating results show that the spar with an optimized composite design has a lighter weight than the original design by around 43%, while it can withstand the same loads with no analytical failure.

Keywords: Aircraft structural design, Seaplane, Composite material, Classical lamination theory, Mechanical properties

INTRODUCTION

Polymer composites are crucial in the aerospace industry, primarily attributable to their reduced mass and exceptional mechanical characteristics. [1]. These materials are thoroughly integrated into structural frameworks such as wings, fuselage, and tail regions, where their exceptional strength-to-weight ratio greatly elevates structural integrity and total performance [2-7]. Furthermore, carbon fiber/epoxy composites have attained notable prominence in commercial aviation, signifying progressive advancements in composite materials since the mid-20th century. Weight reduction represents another critical application, as aircraft with diminished mass contribute to enhanced fuel efficiency and lower operational expenditures, which is essential for promoting sustainability within the aviation sector. In addition, the resistance of polymer composites to corrosion is quite impressive, helping to enhance the longevity of aircraft components while cutting down on maintenance expenditures [4, 8]. In flight-control mechanisms, polymer-based composites are employed in bearings, whose tribological characteristics are paramount across diverse operational scenarios. In summary, incorporating polymer composites within the aerospace sector improves performance metrics and contributes to sustainability objectives by curtailing carbon emissions through optimized design and manufacturing methodologies. Additionally, the evolution of fabrication processes, including additive techniques, is streamlining the production of sophisticated forms and personalized elements, boosting the effectiveness of polymer composites in aircraft design [9].

Generally, for aircraft wings, the main component that carries most of the load produced from the aerodynamics is the wing spar [10]. A two-seater, mono-wing seaplane with an empty weight of 470 kg and a maximum takeoff weight of 650 kg was designed with composite material to reduce the weight and ease of manufacturing. The wing is connected to a wing strut at a distance from the mid-plane of 2.588 m. The strut shares the load from the wing spar and reduces the tip deflection. Figure 1 (a)

DOI: 10.60101/jarst.2024.257706

JOURNAL OF APPLIED RESEARCH ON SCIENCE AND TECHNOLOGY

shows the half-wing planform, wing component (spar, rib, control surfaces), and the strut connecting position. The aircraft wing spar was designed as an I-beam, as the section shown in Figure 1(b).

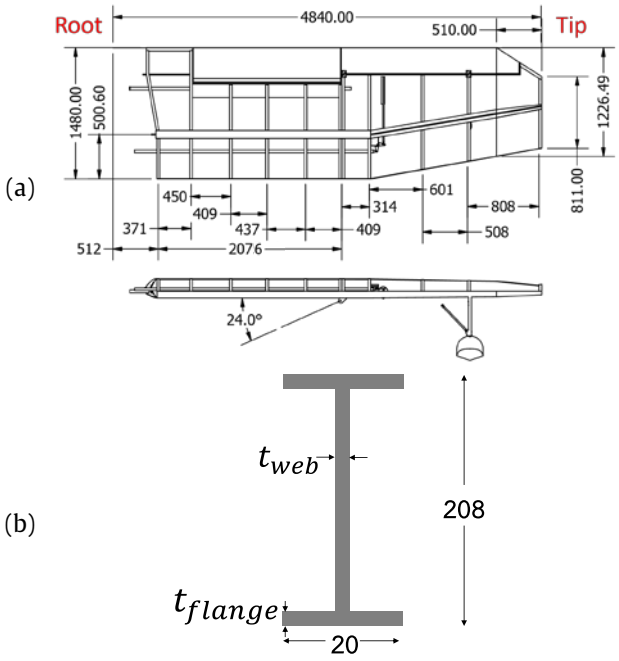

Figure 1 (a) Drawing of the wing (top and front view); (b) spar I-beam cross section at the root (all units in mm).

This work begins by reporting the mechanical properties of the materials utilized in this structure, particularly carbon fiber-epoxy (CF) and glass fiber-epoxy (GF), based on results obtained by material testing according to ASTM standards for composite material. The structural design of composite materials is then provided by an analytical method based on classical lamination theory, which considers three factors: stiffness, strength, and stability (plate buckling) [11]. This method applies the structural calculation of the isotropic material. However, it needs an additional consideration to the material orientation as the composite material is an orthotropic material that can design the ply orientation to counter such load in such direction.

The most appropriate design for the wing spar is finally proposed using the analytical calculation based on Classical lamination theory [11]. Its physical (weight and thickness) and structural safety under the maximum load are compared to the original design.

MATERIALS AND METHODS

Materials

Two materials were used in this study: carbon fiber-epoxy (CF) and glass fiber-epoxy (GF). Carbon fiber is Neotech EC3C60 - carbon 3k plain weave [12], Glass fiber is Fiberglass Cloth EW200 [13], and epoxy is Epotec YDL579 with TH8377M hardener [14]. CF and GF were fabricated with the hand layup method, laying the fiber fabric on a flat aluminum mold and applying epoxy resin ply-by-ply until reaching eight plies (an estimated thickness of 2.5 mm). The hand-laid composite was then covered with vacuum bag and applied with a vacuum pressure. It was left for curing at 44°C for 8 hours. The cured laminates were cut to the recommended size according to ASTM D3039 for tensile testing and ASTM D3518 for in-plane shear properties testing. There are five specimens per testing group. The cut specimens were measured for their width and thickness using a vernier caliper and micrometers, respectively, to report the cross-section size of the specimen for stress calculation. The specimens were tested with a universal testing machine attached to a bi-axial extensometer (Epsilon model 3560-BIA). The force and extension of the specimens were recorded and analyzed for the stiffness, strength, and Poisson's ratio of the materials. The average material properties of both materials are shown in Table 1.

Table 1 CF and GF mechanical properties.

Mechanical properties	CF	GF
Ply thickness (mm)	0.28	0.21
Density (g/cm^3)	1.37	1.61
Fiber volume ratio (%)	41	39.5
Tensile modulus, E_1=E_2 (GPa)	44.81	14.23
Tensile Strength, σ^*_{1T}=σ^*_{2T} (MPa)	467.46	329.78
In-plane shear modulus, G_{12} (GPa)	3.14	2.50
In-plane shear strength, τ_{12} (MPa)	65.71	66.87

Calculation sequence

The composite structure calculation is based on materials' mechanics, *e.g.,* axial, bending, shear stress, and buckling. However, it is slightly different from isotropic material, *i.e.,* aluminum or steel, as composite materials are anisotropic materials that generally have different properties in each direction. The composite wing spar structure is calculated following classical lamination theory, as shown in the diagram in Figure 2. The calculation sequences are:

- Load calculations: The calculation starts from the load calculation, which consists of loads from aerodynamic, structure weight, and attachment on the wing (strut in this case). The ultimate load is identified according to light sport aircraft standard ASTM F2245 [15].
- Initial plies calculation: The initial layup is computed by simplifying the problem to a single load case assuming the equivalent and separately estimating the material required for flange and web by neglecting any interaction between the two components.
- Construct layup: The initial plies requirement will be the initiation of building a laminate for the flange and web. The composite laminate guidance [16] will be considered in this lamination.

DOI: 10.60101/jarst.2024.257706

- Refine calculation: After the laminate with the layup guidelines is constructed, the detailed (refined) calculation, including tip deflection, stress on flange and web, and the buckling, will be calculated for the overall section at the highest load position. The reserve factor (RF) will then be calculated for any possible failure, stress using maximum stress criteria, stability using critical buckling load, and tip deflection limit.
- If the failure occurs in a ply (RF<1), the layup will redesigned by adding plies of materials to avoid a failure.
- If no failure occurs (RF>1): this refers to overdesign and a redundant weight. This leads to removing plies until the lowest RF value among all conditions is just above 1. This laminate will be called an "Optimized layup".

To make the analytical calculation possible, some details of the preliminary design spar were suppressed to simplify the analysis, and there are general assumptions made for the calculation following:

- Straight spar from the root to tip, no bent shape.
- A small off-center of the load from the centroid of the spar leads to negligible torsional load and twist angle.
- Separately calculate the components: top flange, bottom flange, and web, no bonding, curves, or bent joint to be considered.
- The thin wall assumption was applied to all calculations.
- A strut hinge is a point load acting in the strut fixture direction. It can cause some downward load for the deflection calculation.

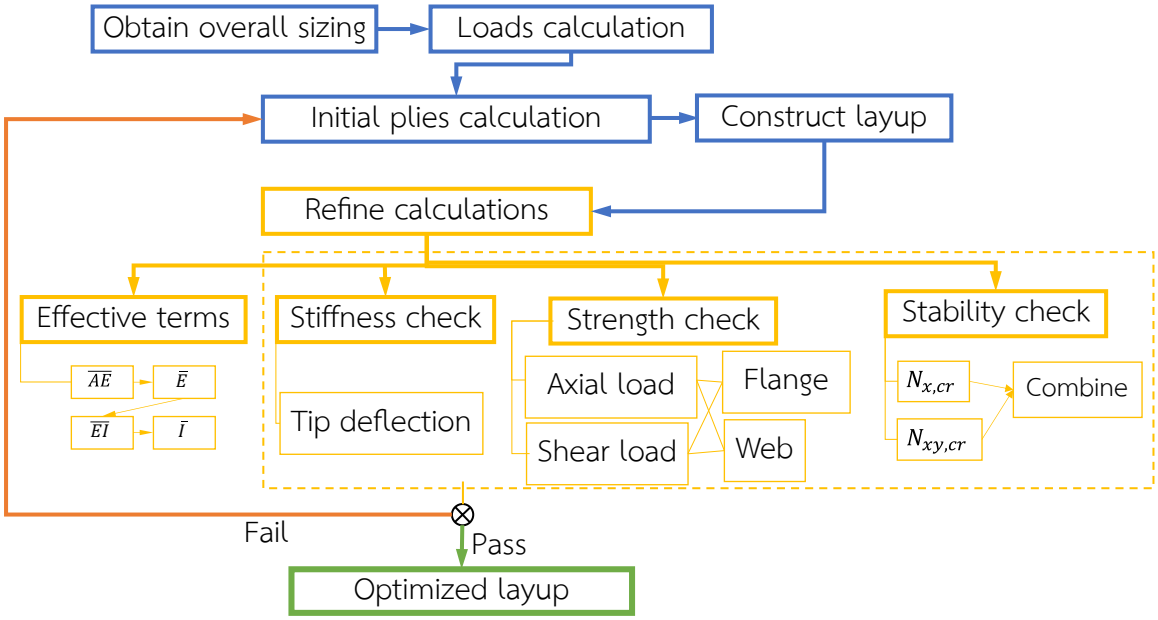

Figure 2 Calculation step for optimized composite laminate design.

Wing loading

The airload (aerodynamic load) along the spanwise was initially calculated according to trapezoid lift distribution [17]. The total lift equals the maximum takeoff weight of the aircraft (650 kg). The dead weight of the wing (50 kg) distributed along the spanwise corresponding to the chord of the section (Figure 1(a)) was deducted from the airload for the total distributed load. The equilibrium force equation calculated the reaction force at the strut hinge point. The distributed load and strut hinge force on the wing are shown in Figure 3(a).

The axial load, shear load, and bending moment diagram were then developed on the wing spar. The critical position of the diagram, located at the strut fixing point (X = 2.588 m), allowed for determining the maximum axial force, shear force, and bending moment. As shown in Figure 3(b), (c), and (d), the maximum axial load (F), shear force (V), and bending moment (M) are, respectively, 5350 N, 1231 N, and 1186 N-m. The ASTM F2245 [15] light sport aircraft load factor (n_{max}=+4) and the safety factor 1.5 at the maximum load were multiplied by the maximum loads from the diagrams.

Initial calculation

Every component (flange and web) had its original estimate of the necessary plies considered. A single-ply orientation-0° plies to counteract axial load on the flange and 45° plies to counteract shear loading in the web-was used to support the load. The basic diagram utilized in the initial computation, the axial stress and shear stress, is shown in Figure 4, where n_x denotes the number of piles in x direction and t_x is the thickness of each pile in the x direction.

DOI: 10.60101/jarst.2024.257706

JOURNAL OF APPLIED RESEARCH ON SCIENCE AND TECHNOLOGY

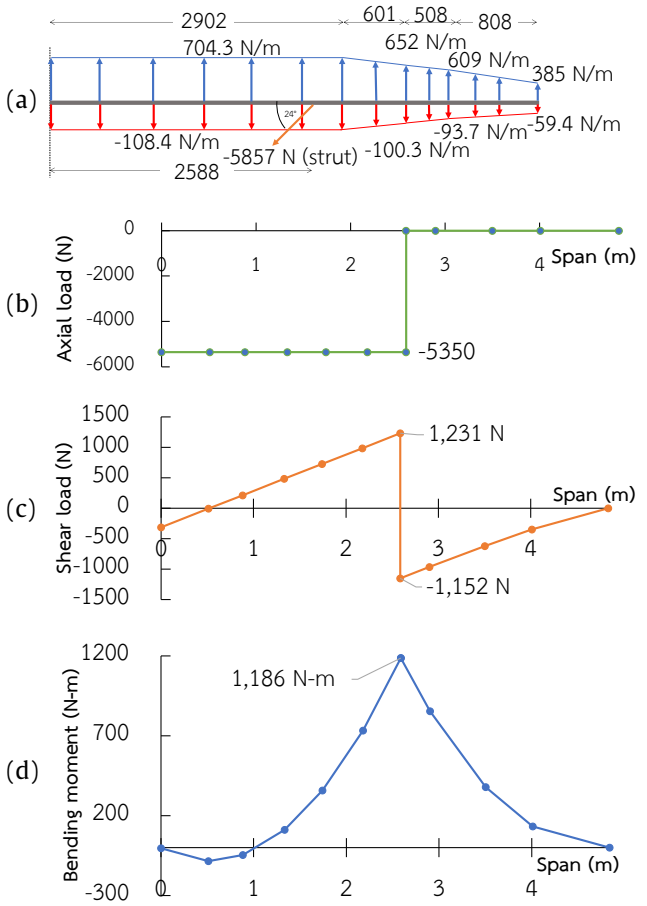

Figure 3 Diagram of (a) wing load distribution, (b) shear, (c) axial force (d) bending moment along the spanwise.

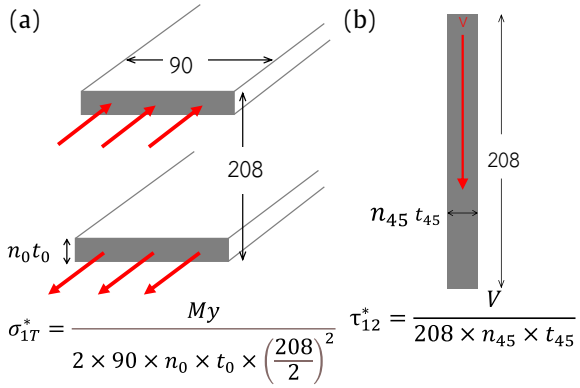

Figure 4 Initial calculation for (a) spar flange 0° plies thickness to counter axial load; (b) spar web 0° plies 45° plies thickness to counter shear load.

Design of the laminate

The laminate will be constructed based on the composite layup guidelines [16]:

- Keep the orientation simple: strict with 0°, 45°, and 90° for the ease of ply cutting.
- Every laminate should have a minimum of 10% of fibers in each direction [0°/±45°/90°] to counter the unpredicted loads.
- Avoid grouping more than 4 plies of the same orientation to minimize the delamination and protect the main load carrying 0° plies.
- The plies drop from the flange to the web needs to be reasonable and possible for manufacturing.

Refine check

There are three checks in the refined calculation: tip deflection (based on composite stiffness), strength, and stability (based on plate bucking). Three of them are based on effective section stiffnesses ($\overline{AE}, \overline{EI}$) and equivalent isotropic section properties ($\bar{E}, \bar{I}$), following equations (1)-(4). The laminate longitudinal stiffness (E_{x_i}) is calculated on each component (flanges and web) separately using ElamX software based on classical lamination theory [18]. A_i and I_i is the area and second moment of inertia of each component (flange and web).

Due to the classical lamination theory, it is restated that only symmetry and balanced laminates, with no extension-bending coupling, are eligible to be used with these computations. Unsymmetric laminate calculation results will be inaccurate but might provide a conceivable structural safety trend.

$$\overline{AE} = \sum (A_i E_{x_i}) \tag{1}$$

$$\bar{E} = \frac{\overline{AE}}{\sum (A_i)} \tag{2}$$

$$\overline{EI} = \sum (I_i E_{x_i}) \tag{3}$$

$$\bar{I} = \frac{\overline{EI}}{\bar{E}} \tag{4}$$

Stiffness refine-check

The tip deflection is usually computed using the superposition method of the point load gathered from the distributed load using beam theory. This is referred to as the beam's stiffness.

$$v = \sum \left(\frac{P_i l_i^3}{3\overline{EI}_i} + \frac{P_i l_i^2}{2\overline{EI}_i} (L - l_i) \right) \tag{5}$$

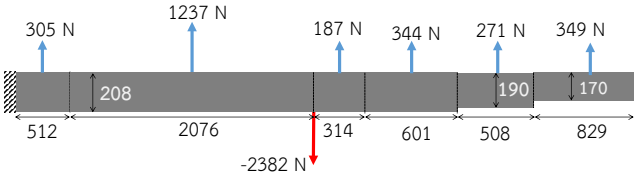

Figure 5 Load case and dimension for tip deflection calculation.

The effect of the spar web taper was simplified to the different section web heights (approximately 208, 190, and 170 mm). Figure 5 displays the theoretical dimension combined with the load case. Equation (5) can be used to calculate the tip deflection (v), which is the result of adding the end load's deflection and the

DOI: 10.60101/jarst.2024.257706

beam's angle after the loading position. P_i is the load at each position, l_i is the length from the root to the load position and L is the total spar length.

Strength check

The stress calculation in this section emphasizes the strut hinge point, X=2.588 m from the wing root, which is the location experiencing the highest load in this situation. Table 2 displays the maximum axial load (F), shear force (V), and bending moment (M) that were derived from Wing loading. In order to get the ultimate load case, these loads were multiplied by 4 and 1.5. The axial and shear stresses were estimated independently.

Table2 Maximum load at X = 2.588 m.

Axial, F (N)	Bending, M (N-mm)	Shear, V (N)
5350	1186 x 10^3	1230

Each component's maximum axial stress ($\sigma_{i,max}$) is calculated by superposing the axial (compression) stress, compression force (F), and the bending stress, bending moment (M), using equation (6), where y_i is the component's highest point of the spar to the centroid of the I-beam cross-section (104 mm). For thin wall shear flow, equation (7) was used to calculate the maximum shear stress ($\tau_{i,max}$). Then the laminate strength determined by applying the 10% rule was compared to the values of laminate strength, σ_T^* and τ_{xy}^*, found in equations (8) and (9).

60% of the tensile strength is a rule of thumb for compressive strength [19]. Since compressive strength is typically lower than tensile strength, the reserve factor (RF), which illustrates the degree of safety of the structure, was finally evaluated for axial (RF_A) and shear loads (RF_{Sh}) using equations (10) and (11). A structure is safe for the maximum load condition if its RF value is greater than 1.

$$\sigma_{i,max} = \left(\frac{My_i}{\bar{I}} + \frac{F}{\Sigma A}\right)\frac{E_{x_i}}{\bar{E}} \tag{6}$$

$$\tau_{i,max} = \frac{q_{max}}{t_i} = \frac{V}{t_i\bar{I}}\left(\int_0^{s_{max}} t_i y ds\right)\frac{E_{x_i}}{\bar{E}} \tag{7}$$

$$\sigma_T^* = \left(1 \times \frac{t_0}{t} + 0.55\frac{t_{45}}{t}\right)\sigma_{1T}^* \tag{8}$$

$$\tau_{xy}^* = \left(0.1 \times \frac{t_0}{t} + 0.55\frac{t_{45}}{t}\right)\frac{\sigma_{1T}^*}{2} \tag{9}$$

$$RF_A = \frac{0.6\sigma_T^*}{\sigma_{i,max}} \tag{10}$$

$$RF_{Sh} = \frac{\tau_{xy}^*}{\tau_{i,max}} \tag{11}$$

Stability check

The stability check compares the critical buckling stress on the laminate, which depends on its flexural stiffness. ElamX software was utilized to compute the critical buckling load intensity for axial ($N_{x,cr}$) and shear ($N_{xy,cr}$) of each laminate component, based on the ESDU chart [20].

The flange and web support were classified as shown in Figure 6. The flange was regarded as half breadth (45 mm) with three sides of simple support and one side free (no support) as it was an I-beam. The dimension of the plate shown in Figure 6 accounted for the critical load position, X = 2.075 to 2.389 m.

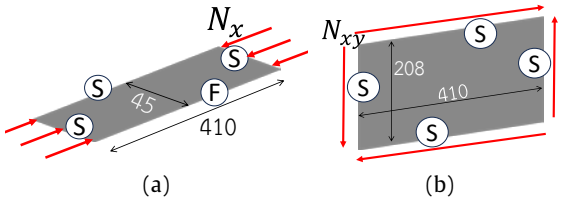

Figure 6 Calculated cases of the (a) buckling on flange; (b) buckling on web (unit in mm).

The stress determined from Section 0 for this section was compared to the critical buckling stress. Equations (12) and (13) were used to determine the RF of each component utilizing the combined loading case of the axial and shear on each component, flange, and web, where t_i is the thickness of the laminate.

$$FI_i = \left(\frac{\tau_{i,max}}{\frac{N_{xy,cr}}{t_i}}\right)^2 + \frac{\sigma_{i,max}}{\frac{N_{x,cr}}{t_i}} \tag{12}$$

$$RF_i = \frac{1}{\sqrt{FI_i}} \tag{13}$$

RESULTS AND DISCUSSION

Initial design

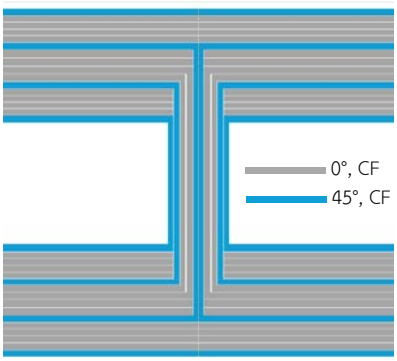

Figure 7 Optimized layup sequence diagram of the design I-beam.

According to the initial calculation in section 0, the initial 0° and 45° plies are 8 and 1 plies, respectively. These make the first layup to $[45, 0_4, \underline{45}]_s$ on the flange and $[45_2, 0_2, 45]_s$ on the web. However, the design results in a low critical buckling load due to the lack of 0° plies on the flanges ($N_{x,cr}$=208 N/mm), which can cause the buckling in the flange due to the axial load.

DOI: 10.60101/jarst.2024.257706

The second design adds a block of four 0° plies to the flanges, which become $[45, 0_4, 45, 0_2]_s$.

As the layup diagram shown in Figure 7, this is referred to as the ply drop from the flange to the web and is considered an optimal design.

Refine calculation

The original design from a publication [21] was compared to the optimal design. It was made from para-beam (P, 4 mm thick) and CF. While the parameters of carbon fiber epoxy in this calculation were based on the available properties in Table 1, the mechanical properties of the para-beam are also obtained from [21]. The layup sequence of the original and optimal designs is shown in Table 3. The spar was designed to be manufactured as a layup of two C-shape beams, followed by an adhesive bonding of the two C-beams back-to-back in the assembly stage with some patching of layers to complete an I-beam with the mentioned laminate. The layup sequence of the two designs was then calculated for their weight by the summation of the spar area and the component thickness multiplied by the density of the composite material. The strength of the laminate was estimated by equations (8) and (9). The practical section stiffnesses and equivalent isotropic section properties were also computed and shown in Table 3. The refined calculation results with the RF for each case of the two designs are shown in Table 4.

Table 3 Refine calculation: layup sequence, dimension, and laminate parameters.

Design	Component	Layup	Thick (mm)	Weight (kg)	E_x (GPa)	Tensile strength (MPa)	Shear strength (MPa)	$\bar{E}$ (GPa)
Optimal (CF only)	Flange	$[45, 0_4, 45, 0_2]_s$	4.48	7.80	39.29	414.8	49.6	35.00
	Web	$[45_2, 0_2, 45]_s$	2.8		28.79	289.8	86.5	
Original (CF + Parabeam)	Top flange	$[0_{12}]_s$	6.72	13.84	45.06	467.5	23.4	28.36
	Web	$[(45,0)_6, \underline{P}]_s$	10.72		21.22	227.1	47.6	
	Btm. flange	$[0_6]_s$	3.36		45.06	467.5	23.4	

Table 4 Refine calculation: stiffness, strength and stability check result.

Design	Component	Stiffness	Stress				Stability		
		Tip Deflection (mm)	Axial stress (MPa)	Shear stress (MPa)	RF axial	RF shear	$N_{x,cr}$ (N/mm)	$N_{xy,cr}$ (N/mm)	$RF_{buckling}$ Combine load
Optimal (CF only)	Flange	213.02	112.27	2.91	2.22	17.08	449.15	858.29	1.09
	Web		50.38	15.44	5.72	5.60	101.40	62.70	1.41
Original (CF + Parabeam)	Top flange	153.74	72.39	2.59	3.87	9.01	562.78	1886.07	1.08
	Web		36.94	4.54	3.69	10.48	3320.22	5393.62	3.82
	Btm. flange		82.54	3.07	5.66	7.62	70.34	235.76	1.11

Comparative discussion

It can be seen that the weight of the optimal design is almost half of the original design, as seen in Table 3. According to the refined calculation check in Table 4, the optimal design has the RF value of flange buckling just above 1 (for both flange-1.09 and web-1.41), indicating the highly optimized design because one case is just at the boundary of the criteria. The original and optimal RF values are more significant than 1, meaning the spars are safe for the ultimate load case. Although both original and optimal designs can pass the refined check with the lowest RF values in similar ranges (1.09 for optimal and 1.08 for the original in the top flange buckling), the original design shows a high stiffness by resulting in a low tip deflection and high strength by showing higher RFs in all strength checks. However, the more robust structure is at the expense of the almost double weight of the spar, which can result in the structure load that can reduce the allowable payload of the aircraft. Moreover, some redundant layers, *e.g.,* 12 plies of 0° in the original web, resulting in a robust structure, *i.e.,* $RF_{buckling,\ web}$ up to 3.82, can be removed to reduce the overall structural weight.

Discussion

The calculation procedure in Figure 2 can provide a reasonable result as the total weight of the design spar is in the same magnitude as the available spar. This implies that the calculation sequence proposed here can be used to design a monolithic structure using composite material with the mentioned assumptions.

DOI: 10.60101/jarst.2024.257706

Although the current method cannot automatically optimize the structure weight, and the designer has to add or remove the ply to obtain the optimal design with the safety criteria, the sequence can be developed further for an automated optimization tool for composite structure design. The tool will not only be limited to the design of aircraft structures, but it can also expand to other lightweight composite structure fields such as automotive parts or civil structures.

According to the assumptions above, the proposed simplified calculation method has some limitations, *e.g.,* the negligible torsional load from the bent shape and off-axis load, which can cause the twisting angle and some additional shear load on the spar. This can change the aerodynamic shape and affect the aerodynamic design. However, the reserve factor for shear load is still high, meaning that the structure should be able to carry the additional shear load without any failure.

Another significant limitation of the calculation method is the assumption of independent component calculation. This was made to calculate the structural stress without any interaction. As a composite material in which the structure was fabricated during manufacturing, the spar structure may have some imperfect bonding, especially at the corners, which can build up a resin pocket or other manufacturing defects, *e.g.,* interlaminar bonding, ply drop or edge ply end, *etc.* These defects can diminish structural strength but cannot be included in the analytical calculation method. Hence, those defect effects were embedded in the safety factor (x1.5) provided before the initial load calculation. The actual spar test must be performed to verify the structural strength and ensure structural safety before entering the line production.

CONCLUSIONS

This article presents an analytical approach for the simplified I-beam wing spar design. It employs orthotropic materials-such as composites-whose computations differ slightly from those of isotropic materials. In order to give the structure the ability to support a particular load in specific directions, it is necessary to consider the ply orientation. It needs consideration of the ply orientation which can assign a specific ply orientation to the structure to carry a specific load in such a direction. Some of the key findings can be concluded as below:

- The calculation for this study was constructed following the classical lamination theory using the mentioned sequence. This can be a guideline for any composite structure design.
- Once the first layup design met the requirements, a layup design aligned with the guidelines was established. The layup was then calculated to determine the ability to withstand the loads and maintain the safety and performance limit. The laminate was then optimized to the minimal requirement of the structure.
- It was found from the calculation sequence that the optimal layup obtained from the calculation sequence is $[45, 0_4, 45, 0_2]_s$ on the flange and $[45_2, 0_2, \underline{45}]_s$ on the web.
- Compared with the original design, this layup is lighter, about 43%, and it complies with basic safety requirements for the mentioned load circumstances. Note that the weight shown in the calculation is only the composite material weight based on the density of composite materials; the actual weight should be slightly more than these figures due to the bonding joint and manufacturing imperfections.

It should be considered that there are some limitations of the suggested method, such as the assumptions of the spar taking a whole load of the aircraft, a perfect bonding of the materials, and a negligible bending spar structure, which could lead to a twisting load. Hence, there should be some potential future work to complete the work as suggested below:

- The twisting of the spar should be included in the detailed torsional load calculation.
- A more detailed calculation should consider the joints of the component, and other components on the wing, including wing ribs and skin, should be included in future calculations.
- Full structural analysis using the finite element method through software should be conducted with a validation of the presented result. This can confirm the overall design of the aircraft.
- Finally, the designed spar and actual full wing, a combination of wing components, must be tested according to the load limit stated in ASTM F2245.

ACKNOWLEDGEMENT

The authors would like to thank Panus Aviation Services Co., Ltd. for assisting with the specimen preparation and providing the aircraft design information.

REFERENCES

1. Awad ZK, Aravinthan T, Zhuge Y, Gonzalez F. A review of optimization techniques used in the design of fibre composite structures for civil engineering applications. Mater Design. 2012;33:534-44.
2. Khames M, Embaby A, Agha A. Comparison between the Use of Aluminum and Composites in the Design of a Wing-Spar of an Airplane. MSF [Internet]. 2019; 953:95-100. Availability from: https://doi.org/10.4028/www.scientific.net/msf.953.95.
3. Kennedy G, Martins JR, editors. A comparison of metallic and composite aircraft wings using

DOI: 10.60101/jarst.2024.257706

aerostructural design optimization. 12th AIAA Aviation Technology, Integration, and Operations (ATIO) Conference and 14th AIAA/ISSMO Multidisciplinary Analysis and Optimization Conference; 2012.

4. Beukers A, Bersee H, Koussios S. Future aircraft structures: From metal to composite structures. In: Nicolais L, Meo M, Milella E, editor. Composite Materials. London: Springer; 2011. p. 1-50.
5. Kesarwani S. Polymer composites in aviation sector. Int J Eng Res. 2017;6(10):518-25.
6. Williams TS. Multifunctional polymers and composites for aerospace applications [Internet]. National Aeronautics and Space Administration; 2019 [cited 2024 Jun 15]. Availability from: https://ntrs.nasa.gov/api/citations/20190026444/downloads/20190026444.pdf
7. Naidu CG, Ramana CV, Rao YS, Rao KVP, Vasudha D, Anusha G, et al. A Concise Review on Carbon Fiber-Reinforced Polymer (CFRP) and Their Mechanical Significance Including Industrial Applications. In: Rahman MM, Asiri AM, Chowdhury MA, editor. Carbon Nanotubes-Recent Advances, New Perspectives and Potential Applications. 2023.
8. Rathod VT, Kumar JS, Jain A. Polymer and ceramic nanocomposites for aerospace applications. Applied Nanoscience. 2017;7:519-48.
9. McIlhagger A, Archer E. Polymer Composites in the Aerospace Industry. 3 Manufacturing processes for composite materials and components for aerospace applications. Woodhead Publishing; 2014. p. 53.
10. Fleuret C, Andreani AS, Lainé É, Grandidier JC, L'héritier S, Gorge AL. Complex wing spar design in carbon fiber reinforced composite for a light aerobatic aircraft. Mech Ind. 2016;17(6):614.
11. Daniel IM, Ishai O, Daniel IM, Daniel I. Engineering mechanics of composite materials. New York: Oxford university press; 1994.
12. Neotech Composites. Carbon plain [Internet]. 2023 [cited 2024 Apr 24]. Availability from: https://neo.co.th/en/products/item/Carbon-plain/carbon-plain.
13. RIGHT Composite. Fiberglass Cloth EW200 [Internet]. 2023 [cited 2024 Apr 24]. Availability from: https://www.rightcomposite.com/EW200-fiberglass-cloth.com.
14. Aditya Birla Chemicals. Epotec Epoxy Systems [Internet]. 2024 [cited 2024 Apr 24]. Availability from: https://www.adityabirlachemicals.com/pdf/Composite.pdf.
15. ASTM International. Standard Specification for Design and Performance of a Light Sport Airplane. ASTM F2245-20 [Internet]. 2020 [updated: 2023 Aug 08; cited 2024 Jan 25]. Availability from: https://cdn.standards.iteh.ai/ samples/107349/078af7bc9da34bc1a892c35efed2c727/ASTM-F2245-20.pdf
16. Abbott R. Analysis and design of composite and metallic flight vehicle structures. 2nd ed. Collingwood: Abbott Aerospace SEZC Ltd; 2016.
17. Corke TC. Design of Aircraft. 1st ed. Pearson; 2003.
18. Hauffe A. ELAMX² [Internet]. Technische Universität Dresden; 2023 [cited 2023 Nov 30]. Availability from: https://tu-dresden.de/ing/maschinenwesen/ilr/lft/elamx2/elamx?set_language=en.
19. Latifi M. Engineered Polymeric Fibrous Materials. Woodhead Publishing; 2021.
20. Markit IHS. ESDU Catalogue 2017 Validated Engineering Design Methods. 2017.
21. Chinvorarat S, Watjatrakul B, Nimdum P, Sangpet T, Soontornpasatch T, Vallikul P. Static testing for composite wing of a two-seater seaplane. IOP Conf Ser: Mater Sci Eng. 2019;501(1):012026.

DOI: 10.60101/jarst.2024.257706